

1 **Deposit-feeding of *Nonionellina labradorica* (foraminifera) from an**  
2 **Arctic methane seep site and possible association with a**  
3 **methanotroph**

4 Christiane Schmidt<sup>1,2,3</sup>, Emmanuelle Geslin<sup>1</sup>, Joan M Bernhard<sup>4</sup>, Charlotte LeKieffre<sup>1,5</sup>, Mette  
5 Marianne Svenning<sup>2,6</sup>, Helene Roberge<sup>1,7</sup>, Magali Schweizer<sup>1</sup>, Giuliana Panieri<sup>2</sup>

6 <sup>1</sup>LPG, Laboratoire de Planétologie et Géosciences, University of Angers, Nantes Université, Le Mans University  
7 CNRS, LPG, SFR QUASAV, Angers, 49000, France

8 <sup>2</sup>CAGE, Centre for Arctic Gas Hydrate, Environment and Climate, UiT, The Arctic University of Norway, Tromsø,  
9 9010, Norway

10 <sup>3</sup>ZMT, Leibniz Centre for Tropical Marine Research, Bremen, 28359, Germany

11 <sup>4</sup>Woods Hole Oceanographic Institution, Geology & Geophysics Department, Woods Hole, 02543, MA, USA

12 <sup>5</sup>Cell and Plant Physiology Laboratory, CNRS, CEA, INRAE, IRIG, Université Grenoble Alpes, Grenoble, 38054  
13 France

14 <sup>6</sup>Department of Arctic and Marine Biology, UiT, The Arctic University of Norway, Tromsø, 9037, Norway

15 <sup>7</sup>Université de Nantes, CNRS, Institut des Matériaux Jean Rouxel, IMN, Nantes, 44000 France

16

17 *Correspondence to* Christiane Schmidt [christiane.schmidt@leibniz-zmt.de](mailto:christiane.schmidt@leibniz-zmt.de)

18

19

20 **Abstract.** Several foraminifera are deposit feeders that consume organic detritus (dead particulate  
21 organic material with entrained bacteria). However, the role of such foraminifera in the benthic  
22 food-web remains understudied. Foraminifera feeding on methanotrophic bacteria, which are  $^{13}\text{C}$ -  
23 depleted, may cause negative cytoplasmic and/or calcitic  $\delta^{13}\text{C}$  values. To test whether the  
24 foraminiferal diet includes methanotrophs, we performed a short-term (20-h) feeding experiment  
25 with *Nonionellina labradorica* from an active Arctic methane-emission site (Storfjordrenna,  
26 Barents Sea) using the marine methanotroph *Methyloprofundus sedimenti*, and analyzed *N.*  
27 *labradorica* cytology via Transmission Electron microscopy (TEM). We hypothesized that *M.*  
28 *sedimenti* would be visible post experiment in degradation vacuoles, as evidenced by their  
29 ultrastructure. Sediment grains (mostly clay) occurred inside one or several degradation vacuoles  
30 in all foraminifers. In 24% of the specimens from the feeding experiment degradation vacuoles  
31 also contained bacteria, although none could be confirmed to be the offered *M. sedimenti*.  
32 Observations of the apertural area after 20-h incubation revealed three putative methanotrophs,  
33 close to clay particles, based on bacterial ultrastructural characteristics. Furthermore, we noted the  
34 absence of bacterial endobionts in all examined *N. labradorica* but confirmed the presence of  
35 kleptoplasts, which were often partially degraded. In sum, we suggest that *M. sedimenti* can be  
36 consumed via untargeted grazing in seeps and that *N. labradorica* can be generally classified as a  
37 deposit feeder at this Arctic site.

38

39 benthic foraminifera – feeding experiment – grazing - marine methanotrophs – Arctic methane  
40 seeps– transmission electron microscopy – ultrastructure – kleptoplasts- protist – molecular  
41 identification

## 42 **1. Introduction**

43 In methane seep sites, the upward migration of methane affects the pore-water chemistry of near-  
44 surface sediments, where benthic foraminifera live (e.g. Dessandier et al., 2019). Extremely light  
45 isotopic signals of  $\delta^{13}\text{C}$  have been measured in seep-associated foraminiferal calcite tests (Wefer  
46 et al., 1994; Rathburn et al., 2003; Hill et al., 2004b; Panieri et al., 2014). Studies specifically  
47 looking at living (bengal rosa stained) foraminiferal tests support the hypothesis that the carbon  
48 isotopic composition is strongly influenced by the porewater DIC (McCorkle et al., 1990a).  
49 Interspecific  $\delta^{13}\text{C}$  differences between species with similar depth indicate sometimes taxon-  
50 specific “vital” effects (McCorkle et al., 1990a). Those “vital” effects describe the biology of the

51 different species, which could reflect different feeding patterns. It has been suggested that  
52 *Nonionella auris* is an indicator of methane release and possibly ingests <sup>13</sup>C-depleted methane  
53 oxidizing bacteria (Wefer et al., 1994). Recently, *Melonis barleeanus* (Williamson, 1858)  
54 collected from an active methane seep site was found to be closely associated with putative  
55 methanotrophs (Bernhard and Panieri, 2018), providing impetus to examine feeding habits of  
56 foraminifera living in or around methane seeps.

57 Methanotrophs produce the biomarker diploptero, which has an extremely light  $\delta^{13}\text{C}$  signature  
58 ( $-60\text{‰}$ ) (Hinrichs et al., 2003). Our hypothesis is that if foraminifera ingest methanotrophs,  $\delta^{13}\text{C}$   
59 values of foraminiferal cytoplasm should be altered by their food. Experiments using a high-  
60 pressure culturing setting illustrated the difficulty to measure the sensitive relationship between  
61 methane exposure and the foraminifera *Cibicides wuellerstorfi*. However, it was shown in one  
62 experiment using entire cores that a methane source was reflected in  $\delta^{13}\text{C}$  of foraminiferal calcite  
63 (Wollenburg et al., 2015). It is also not yet conclusive if the food can influence foraminiferal  
64 calcite, as foraminifera sometimes fail to produce new calcite in experiments (Mojtahid et al., 2011).  
65 Another hypothesis to explain extremely light  $\delta^{13}\text{C}$  values recorded in benthic foraminiferal calcite  
66 is that foraminifera assimilate carbon as <sup>13</sup>C-depleted methane-derived DIC, which would lead to  
67 extremely light  $\delta^{13}\text{C}$  values. The possibility that <sup>13</sup>C-depleted DIC from the pore water can be  
68 assimilated by foraminifera is currently debated. Some studies suggest it is not possible (Herguera  
69 et al., 2014), while others assert the feasibility that foraminifera calcify close to seeps (Rathburn  
70 et al., 2003; Hill et al., 2004a; Panieri et al., 2014). The problem lies in the calcite tests, and the  
71 difficulty to assess the time of death of these protists in the sediment. Several studies found that the  
72 lightest isotopic  $\delta^{13}\text{C}$  values were measured in tests coated by methane-derived authigenic  
73 carbonate (MDAC) overgrowth, which happens after the death of the foraminifer (Torres et al.,  
74 2010; Panieri et al., 2014; Consolaro et al., 2015; Panieri et al., 2017; Schneider et al., 2017).  
75 However, light  $\delta^{13}\text{C}$  values remain in many tests after MDACs are removed (Panieri et al., 2014)  
76 and have been measured also in primary calcite, without MDACs, from tests in methane-rich  
77 environments (e.g. Mackensen, 2008; Dessandier et al., 2019). These observations again point to  
78 the role of food influencing the cytoplasmic  $\delta^{13}\text{C}$ .

79 Foraminifera play an important role in the carbon cycle on the deep seafloor (Nomaki et al., 2005)  
80 where feeding behavior and food preference vary with species (Nomaki et al., 2006). Selected  
81 species of deep-sea benthic foraminifera have been shown to feed selectively on <sup>13</sup>C-labeled algae

82 from sedimentary organic matter, but unselectively on  $^{13}\text{C}$ -labeled bacteria of the strain *Vibrio*  
83 (Nomaki et al., 2006). A study from the seafloor around Adriatic seeps suggested that  $\delta^{13}\text{C}$  of  
84 foraminiferal cytoplasm could be influenced by feeding on the sulfur-oxidizing bacterium  
85 *Beggiatoa*, whose abundance was also positively correlated with foraminiferal densities (Panieri,  
86 2006). Generally, some foraminifera can ingest dissolved organic matter (DOM); some are  
87 herbivorous, carnivorous, suspension feeders and most commonly deposit feeders reviewed in  
88 (reviewed in Lipps, 1983). Deposit feeders are omnivorous, gathering fine-grained sediment (e.g.,  
89 clay) and associated bacteria, organic detritus (dead particulate organic material) and, if present,  
90 diatom cells using their pseudopodia. Based on the ultrastructure of the diet found in vacuoles  
91 several species of foraminifera from different habitats have already been classified to be deposit  
92 feeders (Goldstein and Corliss, 1994).

93 Here we investigate if *Nonionellina labradorica* would feed in a short-term feeding experiment on  
94 the marine methanotroph *Metyloprofundus sedimenti* and compare its ultrastructure on  
95 experimental specimens and field specimens. *Nonionellina labradorica* is an abundant species in  
96 the North Atlantic (Cedhagen, 1991) and occurs together with *N. digitata* in Svalbard fjord  
97 sediments (Hald and Korsun, 1997; Shetye et al., 2011; Fossile et al., 2020). In addition to its wide  
98 distribution, it is an especially interesting experimental species for feeding studies because it hosts  
99 kleptoplasts, *i.e.* sequestered chloroplasts, of diatom origin inside its cytoplasm (Cedhagen, 1991;  
100 Jauffrais et al., 2019b). *Nonionellina labradorica*'s aperture shows a specific ornamentation,  
101 possibly a morphological adaptation to this "predatory" mode of life for obtaining the kleptoplasts  
102 (Bernhard and Bowser, 1999). Denitrification has been speculated for *N. labradorica* (reviewed  
103 in Charrieau et al., 2019), because the foraminiferal genus *Nonionella* can denitrify, which was  
104 demonstrated on two species (Risgaard-Petersen et al., 2006; Choquel et al., 2021), but not yet on  
105 *N. labradorica*. Our study analyzed contents of the degradation vacuoles of this species from an  
106 active methane-emitting site in the Arctic (Storfjordrenna, Barents Sea) before and after a feeding  
107 experiment.

## 108 **2. Materials and methods**

### 109 **2.1. Site description and sampling living foraminifera**

110 The sampling site was located app. 50 km south of Svalbard at 382m water depth at the mouth of  
111 Storfjordrenna (Serov et al., 2017). The site is characterized by several large gas hydrate pingos

112 (GHP), which actively vent methane over an area of 2.5 km<sup>2</sup>. Our samples were taken at GHP3,  
113 which is referred to as an underwater gas hydrate-bearing mound (Hong et al., 2017; Hong et al.,  
114 2018). GHP3 is a ~500-m diameter, 10-m tall mound that actively vents methane (Fig. 1). Marine  
115 sediment samples were collected during CAGE cruise 18-05 supported by the research vessel  
116 *Kronprins Haakon* on October 2018 and sampled by the Remotely Operated Vehicle (ROV) *Ægir*.  
117 A blade corer (surface dimensions 27 x 19 cm, Fig. 1c) was used to sample living foraminifera; it  
118 was placed directly in the vicinity of bacterial mats. The blade corer containing the sediment  
119 sample was opened immediately once onboard. A small aquarium hose was used to sample the  
120 upper most surface layer (0-1 cm). The wet sediment was collected in petri dishes and wet sieved  
121 to a size range of 250-500 µm, which served as source of living (cytoplasm containing)  
122 foraminifera. The species *N. labradorica*, which was abundant, was subsequently used for a  
123 feeding experiment described in detail below.

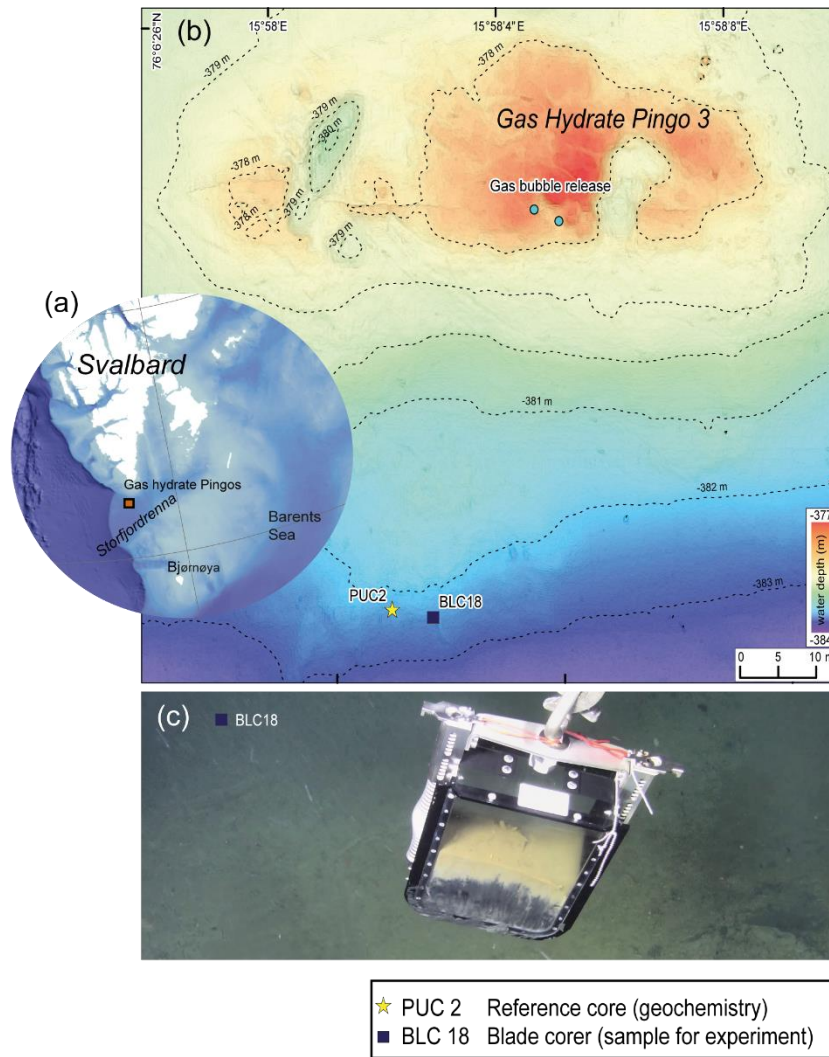


**Figure 1. Description of the sampling site Gas hydrate Pingo 3 (GHP3), a gas-hydrate bearing mound, located in Storfjordrenna Barents Sea. (a) Map illustrating Svalbard Archipelago and the the sampling site, app. 50 km offshore. (b) Map of sampling site GHP3, active gas bubble release is marked on the top of the underwater mount, yellow star indicates location of push corer PUC2 (geochemical analyses), black square indicates location of BLC18 (sediment source for experiment). (c) Underwater image of retrieval of BLC18 taken by ROV camera illustrating the coloration of sediment with the sea-floor visible in background.**

## 125 **2.2. Geochemistry of the study site**

126 For geochemical analysis of the study site a push corer (PUC2; from now referred to as  
127 geochemistry core) was taken to obtain measurements of  $\delta^{13}\text{C}_{\text{DIC}}$  and sulfate, because blade corer  
128 (BLC18) did not allow those measurements. PUC2 was taken in close vicinity to BLC18, ~5m  
129 apart (see Figure S1). Pore-water samples were taken from PUC2 using rhizons that were inserted  
130 through pre-drilled holes in the core tube at intervals of 1 cm (Table S1). Acid washed 20-ml  
131 syringes were attached to the rhizons for pore water collection. Depending on the amount of pore  
132 water collected, the samples were split for  $\delta^{13}\text{C}_{\text{DIC}}$  and sulfate measurements. To the samples, 10  
133  $\mu\text{L}$  of saturated  $\text{HgCl}_2$  (aqueous) was added to stop microbial activity and stored in cold conditions  
134 ( $5^\circ\text{C}$ ). A ThermoScientific Gasbench II coupled to a ThermoScientific MAT 253 IRMS at the  
135 Stable Isotope Laboratory (SIL) at CAGE, UiT was used to determine  $\delta^{13}\text{C}_{\text{DIC}}$  of the pore-water.  
136 Anhydrous phosphoric acid was added to small glass vials (volume 4.5 mL), that were closed and  
137 flushed with helium 5.0 gas before the pore-water sub-sample was measured. A pore-water sub-  
138 sample (volume 0.5 mL) was then added through the septa with a syringe needle, followed by  
139 equilibration for 24 h at  $24^\circ\text{C}$  to liberate the  $\text{CO}_2$  gas. Three solid calcite standards with a range of  
140 +2 to -49 ‰ were used for normalization to  $\delta^{13}\text{C}$  -VPDB. Correction of measured  $\delta^{13}\text{C}$  by -0.1 ‰,  
141 was done to account for fractionation between (gas) and (aqueous) in sample vials. Instrument  
142 precision for  $\delta^{13}\text{C}$  on a MAT253 IRMS was  $\pm 0.1$  ‰ (SD). Sulfate was measured with a Metrohm  
143 ion chromatography instrument equipped with column Metrosep A sup 4, and eluted with 1.8  
144 mmol/L  $\text{Na}_2\text{CO}_3$  + 1.7 mmol/L  $\text{NaHCO}_3$  at the University of Bergen.

## 145 **2.3. Culturing of the marine methanotroph *M. sedimenti***

146 *Methyloprofundus sedimenti* PKF-14 had been previously isolated from a water-column sample  
147 collected at Prins Karls Forland, Svalbard in the laboratory at UiT in Tromsø. *Methyloprofundus*  
148 *sedimenti* were cultured in 10-ml batches of a 35:65 mix of 1/10 Nitrate Mineral Salt medium  
149 (NMS) and sterile filtered sea water using 125-mL Wheaton<sup>®</sup> serum bottles with butyl septa and  
150 aluminum crimp caps (Teknolab<sup>®</sup>). Methane was injected to give a headspace of 20% methane in  
151 air, and the bottles were incubated without shaking at  $15^\circ\text{C}$  in darkness. Purity of the cultures and  
152 cell integrity was verified by microscopy and by absence of growth on agar plates with a general  
153 medium for heterotrophic bacteria (tryptone, yeast extract, glucose and agar).

154 Transmission Electron Microscopy was performed on culture aliquots to allow morphological  
155 comparison to previously published work (Tavormina et al., 2015).

#### 156 **2.4. Experimental setup**

157 On the ship, *Nonionellina labradorica* (Fig. 2a,b) specimens showing dark greenish brown  
158 cytoplasm were picked using sable artist brushes under a stereomicroscope immediately after wet  
159 sieving the sediment using natural seawater delivered from the ship pump. Living specimens had  
160 a partly inorganic covering surrounding the test, which was gently removed using fine artist  
161 brushes. Those so-called cysts are nothing unusual with many foraminiferan taxa (Heinz et al.,  
162 2005).

163 Our specimens were subsequently rinsed twice in filtered artificial seawater to remove any  
164 sediment before placing them into the experimental petri dishes. Care was taken that those were  
165 minimally exposed to light during preparation of the experiment, as kleptoplasts are known to be  
166 highly light sensitive in this foraminifer (Jauffrais et al., 2019b).

167 The experiment with *M. sedimenti* was conducted for a total duration of 20-h to resemble previous  
168 experiments on *N. labradorica* using transmission electron microscopy and nanometre-scale  
169 secondary ion mass spectrometry (TEM-NanoSIMS) isotopic imaging, and included two more  
170 time points at 4 and 8 h. A short pre-experimental phase (2-4 h) was included before the start of  
171 the feeding experiment, to allow specimens to acclimate. During the pre-experimental phase  
172 specimens were not fed and resided in the petri dishes to adjust to the experimental conditions.  
173 The feeding experiment consisted of several small petri dishes (3.5 cm Ø, 3 mL) each containing  
174 five *N. labradorica* in ASW at ambient salinity 35 (Red Sea Salt). Petri dishes were sealed with  
175 Parafilm® and covered with aluminum foil and placed inside the incubator in complete darkness.  
176 Temperature inside the chamber was maintained at 2-3°C, which is within the range of the site's  
177 bottom-water temperature (-1.8 – 4.6°C) (Hong et al., 2017). The feeding of *M. sedimenti* was  
178 performed once at the beginning of the experiment by adding 100 µL of culture to 3 mL of artificial  
179 seawater to produce a final concentration of ~1E10<sup>6</sup> bacteria / mL in each petri dish. Previously  
180 conducted feeding studies were used as guides: Muller and Lee (1969) used 1E10<sup>4</sup> bacteria/mL  
181 seawater and Mojtahid et al. (2011) used 4E10<sup>8</sup> bacteria/mL seawater.



182 Five foraminifera, which served as initial/field specimens (Table 1), were fixed without *M.*  
183 *sedimenti* incubation. The respective petri dishes were incubated for 4, 8 and 20 h to determine if  
184 incubation duration influenced response of the foraminifera to the methanotroph. One petri dish  
185 containing five foraminifera, which were un-fed and fixed at 20 h, served as a negative “control”.  
186 After the end of the respective incubation times, each foraminifer was picked with a sterilized fine  
187 artist brush, which was cleaned in 70% ethanol between each specimen, and placed individually  
188 into a fixative solution (4% glutaraldehyde and 2% paraformaldehyde dissolved in ASW).

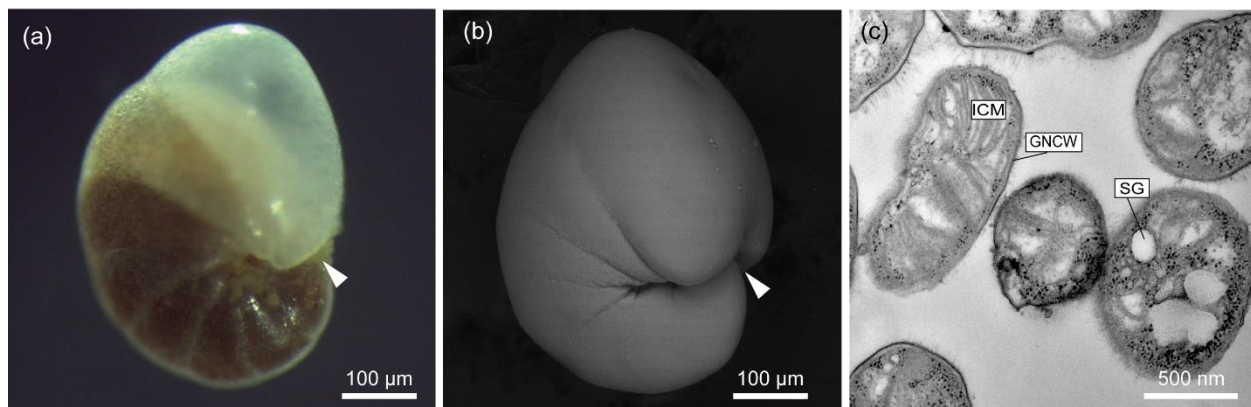


Figure 2 Exemplary illustration of *Nonionellina labradorica*, utilized in this study. (a) Reflected light microscopy image from a specimen directly after sampling, white arrowhead indicates aperture location. (b) Scanning electron image from a specimen before molecular analysis was performed, white arrowhead indicates aperture location. (c) Transmission electron microscopy image of a culture of *Methyloprofundus sedimenti*, the marine methanotroph used in the feeding experiment. The characteristic features for methanotroph identification is the typical type I intracytoplasmic membrane (ICM). Furthermore, other internal structures visible are storage granules (SG), and a gram-negative cell wall (GNCW).

## 189 2.5. Transmission Electron microscopy (TEM) preparation

190 Samples of *N. labradorica* preserved in fixative solution were transported to the University of  
191 Angers, where they were prepared for ultrastructural analysis using established protocols  
192 (Lekieffre et al., 2018). Four embedded foraminiferal cells per treatment were sectioned using an  
193 ultramicrotome (Leica<sup>®</sup> Ultracut S) equipped with a diamond knife (Diatome<sup>®</sup>, ultra 45°). Grids  
194 were stained using UranylLess<sup>®</sup> EM Stain (EMS, USA). Ultra-thin sections (70 nm) were observed  
195 with a JEOL JEM-1400 TEM at the SCIAM facility, University of Angers.

196 To document the ultrastructure of *Methyloprofundus sedimenti*, a sub-sample of the culture used  
197 for experiments was imaged with TEM (Fig. 2c). To do so, an exponentially growing culture was  
198 collected, centrifuged, pre-fixed with 2.5 % (w/v) glutaraldehyde in growth medium overnight,

199 washed in PBS (Phosphate Buffered Saline), then post fixed with 1% (w/v) aqueous osmium  
200 tetroxide for 1.5 hours at room temperature. After dehydration in an ethanol series, the samples  
201 were embedded in an Epon equivalent (Serva) epoxy resin. Ultra-thin sections were cut on a Leica  
202 EM UC6 ultramicrotome, and stained with 3 % (w/v) aqueous uranyl acetate followed by staining  
203 with lead citrate (Reynolds, 1963) at 20 °C for 4–5 min. The samples were examined with a JEOL  
204 JEM-1010 transmission electron microscope at an accelerating voltage of 80 kV with a Morada  
205 camera system at the Advanced Microscopy Core Facility (AMCF), Faculty of Health Science,  
206 UiT The Arctic University of Norway.

## 207 **2.6. Foraminifera ultrastructural observation and image processing**

208 Four specimens per experimental time point (initials, 4, 8 and 20 h) plus one un-fed (control)  
209 specimen were examined with the TEM. From each specimen, a minimum of 50 TEM images was  
210 taken, including images detailing the degradation vacuoles (5-27 images of degradation vacuoles  
211 per specimen). The ultrastructure was examined at different parts of the sections focusing (a) in  
212 the cell interior to document vitality, (b) on degradation vacuoles to determine their content, and  
213 (c) at the exterior to survey for microbes entrained in remnant “reticulopodial trunk” material. All  
214 images made during the observations at the TEM are deposited at PANGAEA (DOI).

## 215 **2.7. Molecular genetics and morphology**

216 DNA metabarcoding and morphological documentation were performed on 13 specimens of *N.*  
217 *labradorica*. Briefly, live specimens were dried on micropaleontological slides and transported in  
218 a small container, cooled with ice-pads to the University of Angers. All specimens were imaged  
219 for morphological analysis using a Scanning Electron Microscope (SEM; EVOLS10, ZEISS, Fig.  
220 S1) followed by individually extracting total DNA in DOC buffer (Pawlowski, 2000). To amplify  
221 foraminiferal DNA, a hot start PCR (2 min. at 95°C) was performed in a volume of 25µl with 40  
222 cycles of 30 s at 95°C, 30 s at 50°C and 2 min at 72°C, followed by 10 min at 72°C for final  
223 extension. Primers s14F3 and sB were used for the first PCR and 30 cycles at an annealing  
224 temperature of 52°C (other parameters unchanged) for the nested PCR with primers s14F1 and J2  
225 (Pawlowski, 2000; Darling et al., 2016). Positive amplifications were sequenced directly with the  
226 Sanger method at Eurofins Genomics (Cologne, Germany). For taxonomic identification, DNA  
227 sequences were compared first with BLAST (Basic Local Alignment Search Tool) (Altschul et al.,

228 1997) and then within an alignment comprising other Nonionids implemented in SeaView (Gouy  
229 et al., 2010) and corrected manually.

### 230 **3. Results**

#### 231 **3.1. Sample description and geochemistry of the study site**

232 The visual observation of the sediments within the blade corer BLC18 immediately after sampling  
233 (Fig. 1c) indicated that the sediment appeared light grey – yellowish in the upper part until app. 13  
234 cm and dark brown from app. 13 cm to the bottom. The sulfate measured in the pore water of the  
235 geochemistry core (PUC2) declined from ~2750 ppm at the sediment-water interface to ~706 ppm  
236 at approximately 13 cm (see Fig. S1, Table S1). A decline in sulfate concentration indicates that  
237 the anaerobic oxidation of methane (AOM) occurred at app. 13 cm depth. The SMTZ (Sulfate  
238 Methane Transition Zone) characterized by a reduced  $\delta^{13}\text{C-DIC}$  -32‰ at app. 13 cm sediment  
239 depth can be considered shallow on the global average (Egger et al., 2018).

#### 240 **3.2. Ultrastructure of methanotroph culture used in the feeding experiment**

241 Transmission Electron Microscopy was performed on culture aliquots to allow morphological  
242 comparison to previously published work (Tavormina et al., 2015). *Methyloprofundus sedimenti*  
243 strain PKF-14 cells appear to have a gram-negative cell wall, coccoid to slightly elongated shape  
244 and characteristic intracytoplasmic membrane (ICM) (Fig. 2c). Additionally, 16S rRNA gene  
245 sequencing was performed (data not shown) to confirm it to be similar to the published  
246 *Methyloprofundus sedimenti* (Tavormina et al., 2015). *Metyloprofundus sedimenti* is characterized  
247 by a typical type I intracellular stacked membrane (ICM). Furthermore, it has storage granules  
248 (SG) and a gram-negative cell wall (GNCW) (Fig. 2).

#### 249 **3.3. Foraminiferal ultrastructure from an Arctic seep environment**

##### 250 **3.3.1 General ultrastructure**

251 All 17 specimen examined for ultrastructure were considered living at the time of observation (Fig.  
252 3), as the mitochondria had characteristic double membranes and occasionally visible cristae  
253 (Nomaki et al., 2016). Cytoplasm exhibited several vacuoles and kleptoplasts concentrated in the  
254 youngest chambers (Fig. 3a) and, in some specimens, the nucleus with nucleoli was visible (Fig.  
255 3b). Kleptoplasts were numerous throughout the cytoplasm and occurred in the form of a single  
256 chloroplast (Fig. 3a-b), or as double chloroplasts (Fig. S2a-d). Not all kleptoplasts were intact;

257 some showed peripheral degradation of the membranes indicated by an increasing number of white  
258 areas between pyrenoid, lamella and thylakoids (Fig. S2a-d). The mitochondria occurred often in  
259 small clusters of two to five throughout the cytoplasm and were oval, round or kidney-shaped in  
260 cross section (Fig. 3e-f). Peroxisomes in *N. labradorica* occurred mostly as pairs (Fig. 3c) or small  
261 clusters of 3-4 spherical organelles (Fig. S3a). Sometimes, but not always, peroxisomes were  
262 associated with endoplasmic reticulum (Fig. S3b) but could also occur alone. Golgi apparatus (Fig  
263 3d) had intact membranes, often occurring near mitochondria.

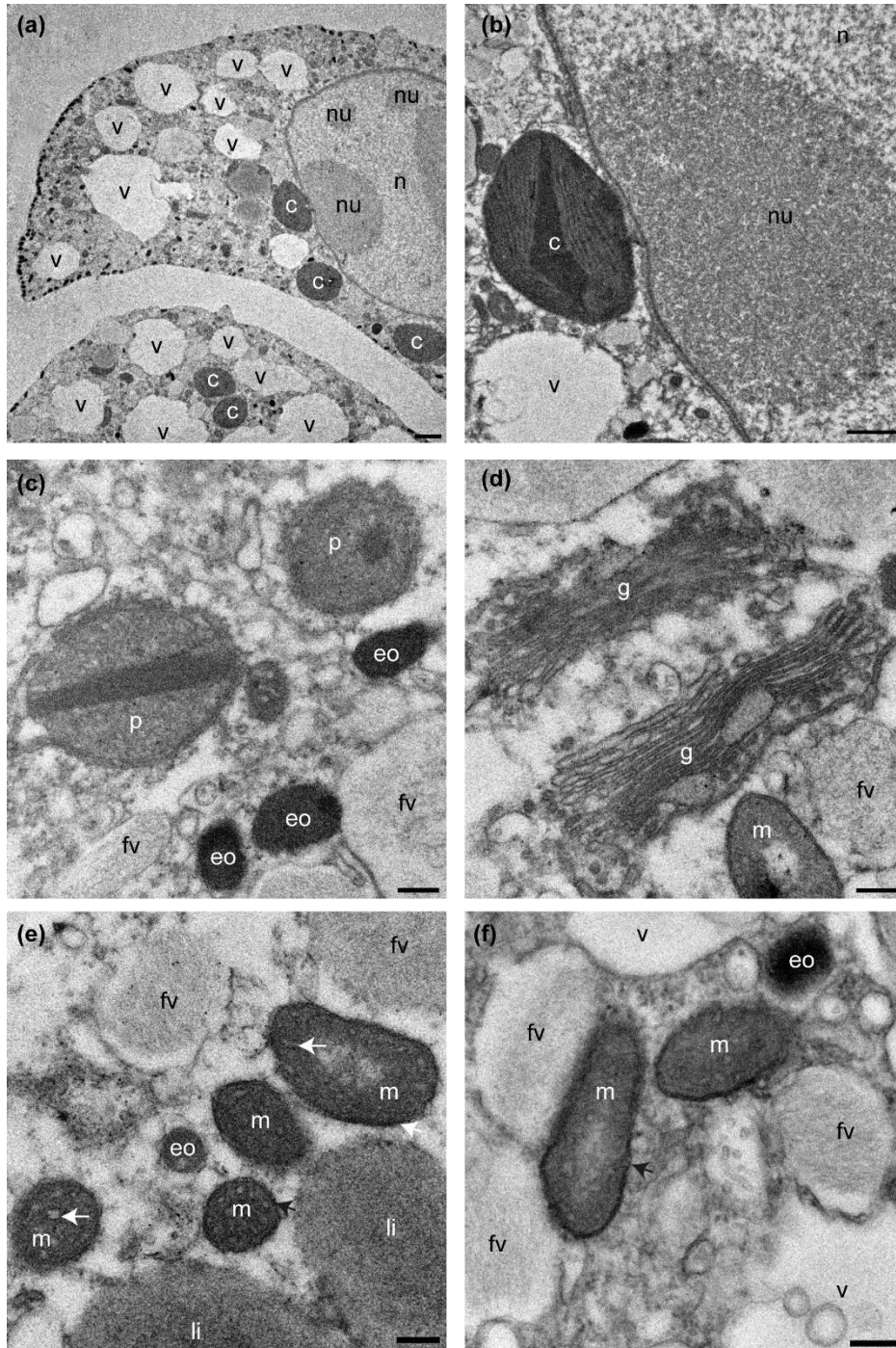


**Figure 3** Transmission electron micrographs showing cellular ultrastructure of *N. labradorica*. (a) Cytoplasm showing parts of two chambers, with nucleus with nucleoli, vacuoles and several kleptoplasts, (b) nuclear envelope, nucleoli, and kleptoplasts, (c) peroxisomes and electron opaque bodies, (d) Golgi, (e-f) mitochondria. V=vacuole, c=kleptoplast, nu=nucleoli, n=nucleus p=peroxisome, eo=electron opaque body, m=mitochondrion, fv=fibrillar vesicle, li=lipid droplet. Scales: (a) 2  $\mu\text{m}$ , (b) 1  $\mu\text{m}$ , (c-f) 200 nm

265 **3.3.2 Ultrastructure of aperture-associated bacteria**

266 In total, three putative methanotrophs were identified in the vicinity of two specimens (sample  
267 E39, Fig. 4; E37, Fig. 5). These microbes were identified next to reticulopodial remains (Fig. 4b).  
268 As an aid for identification of *M. sedimenti* we used the characteristics shown in the literature  
269 (Tavormina et al., 2015) and our own TEM observation obtained from *M. sedimenti* culture (Fig.  
270 2c). As noted, *Methyloprofundus sedimenti* is characterized by a typical type I intracytoplasmic  
271 stacked membrane (ISM). Other characteristics, which are not specific for methanotrophs included  
272 storage granules (SG) and a typical gram-negative cell wall (GNCW) (Fig. 2c). On specimen E39  
273 from the 20 h treatment, we found the methanotroph exhibiting the clearest internal structure,  
274 having both typical type I intracytoplasmic stacked membranes (ISM) and SG, as well found and  
275 a second putative methanotroph showing GNCW and SG (Fig. 4c).  
276

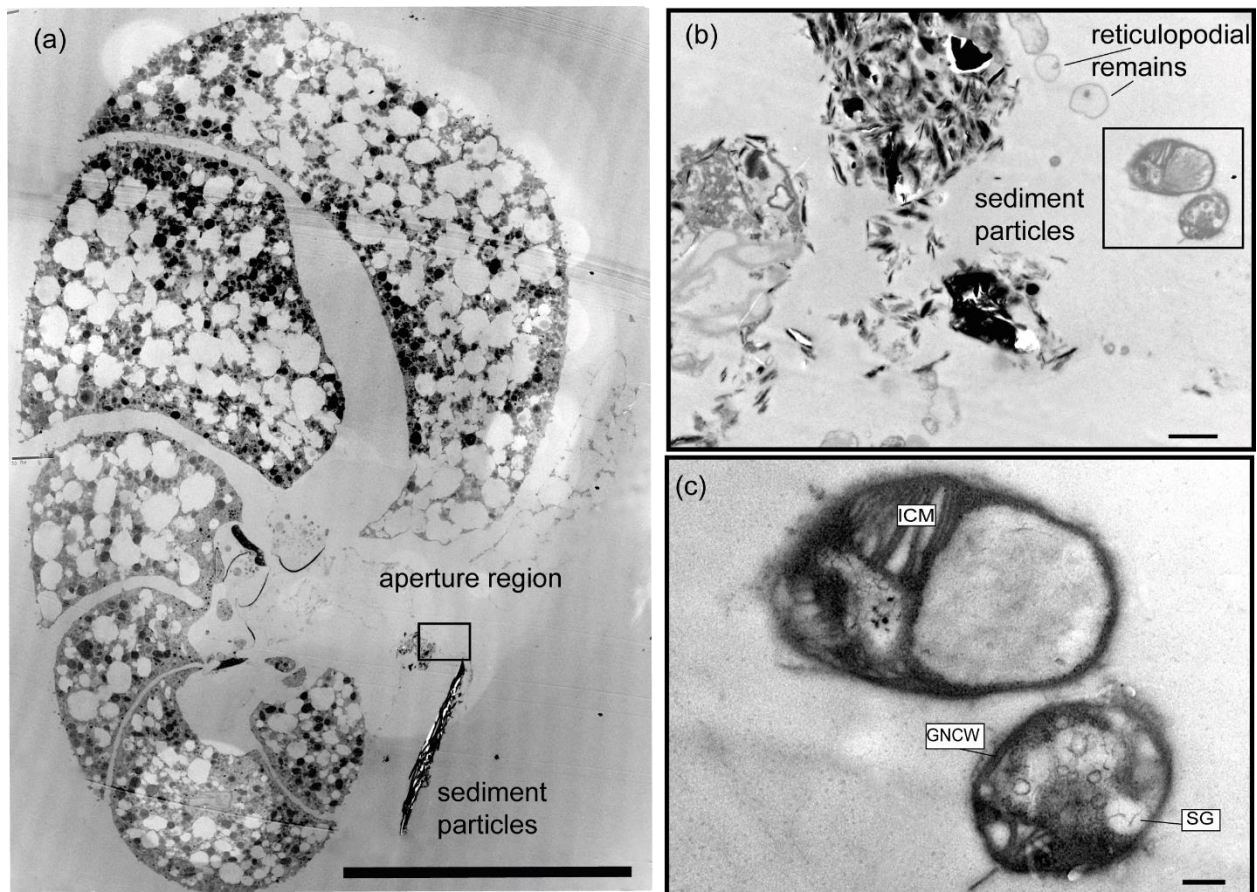
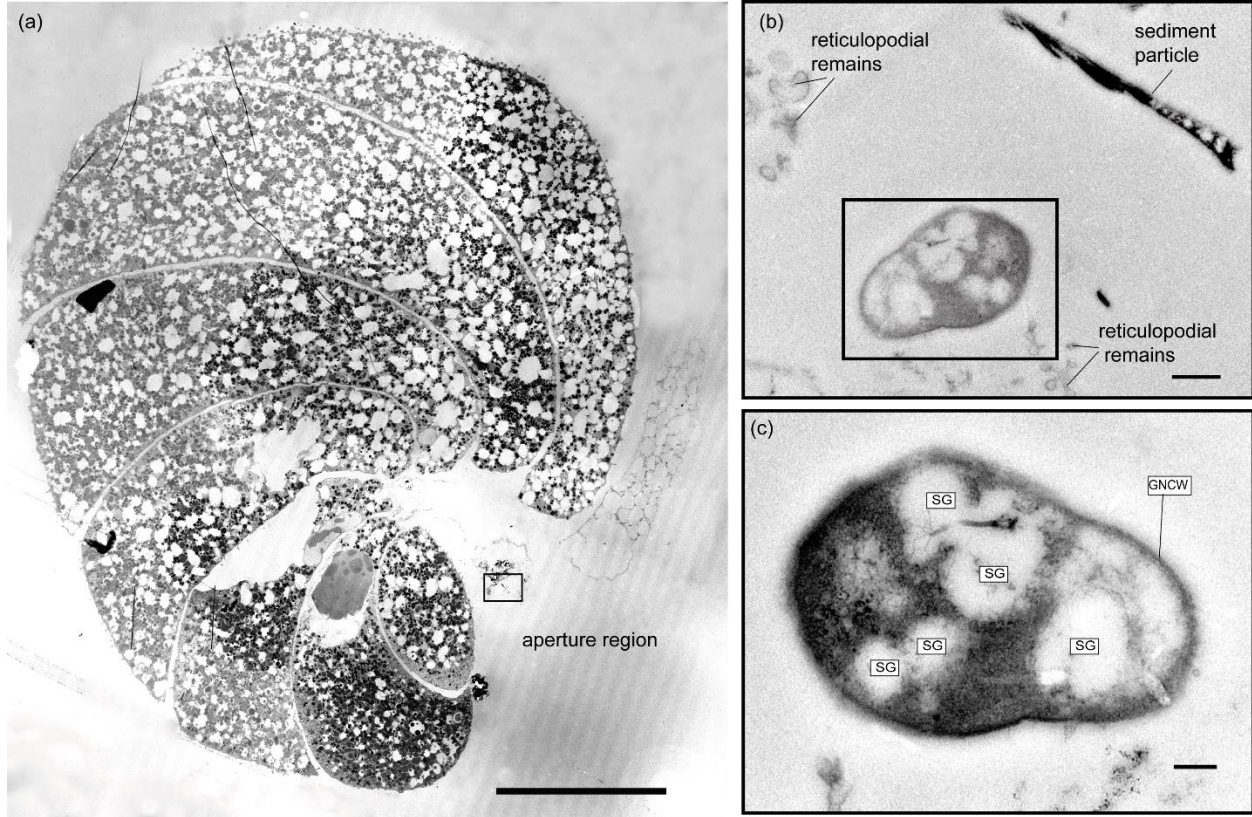


**Figure 4** Transmission electron micrographs of *N. labradorica* from 20 h treatment (sample E39) (a) Stitched cross section of TEM images showing location of methanotroph at the aperture region (black rectangle) (b) Location of two putative methanotrophs next to sediment particles and putative reticulopodial remains. (c) Close up of two putative methanotrophs revealing detailed feature for identification, such as type I stacked intracytoplasmic membranes (ISM), and other less-

informative characteristics, such as storage granules (SG), and gram-negative cell wall (GNCW), scale bars: a: 100  $\mu\text{m}$ , b: 1  $\mu\text{m}$ , c: 200 nm.



277

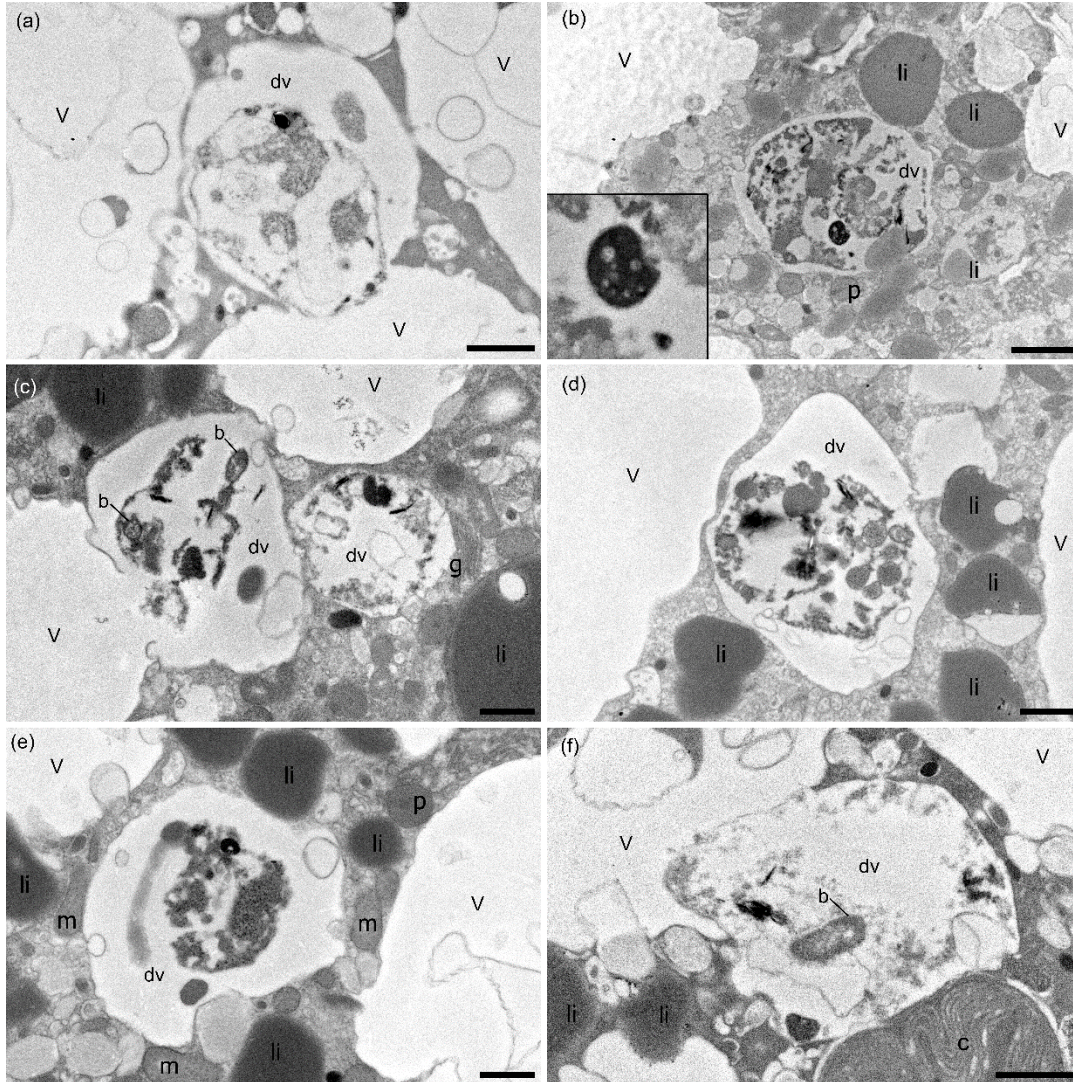
**Figure 5** Transmission electron micrographs of *N. labradorica* from 20 h treatment (sample E37) (a) Stacked cross section of TEM images showing location of putative methanotroph (black rectangle) at the aperture region. (b) Location of the putative methanotroph next to sediment particles and sections of the putative reticulopodial remains (c) Close up of putative methanotroph showing several SG throughout its cell, scale bars: a: 100  $\mu\text{m}$ , b: 0.5  $\mu\text{m}$ , c: 200 nm.

278

### 279 3.3.3 Contents of degradation vacuoles

280 Digestive vacuoles and food vacuoles are often summarized as degradation vacuoles in the  
281 literature (Lekieffre et al., 2018) and this makes sense for our study as well. A degradation vacuole  
282 is a vacuole where enzymatic activities degrade contents, often making them unidentifiable (Bé et  
283 al., 1982; Hemleben et al., 2012). Sediment particles were present in many degradation vacuoles.  
284 The sediment grains were easy to recognize in the TEM image as angular grains inside the  
285 vacuoles, next to organic debris, which can have many different shapes. Each specimen had at  
286 least one and mostly several degradation vacuoles filled with sediment particles (Table 1). If a  
287 sediment particle was visible, the vacuole was defined as a degradation vacuole (dv), and if it was  
288 not and empty then it was defined as a standard vacuole (v) (Fig. 6). The observed entrained  
289 sediment particles were platelets, likely clay from the seafloor, and hence show that the vacuole

290 must contain foreign objects, around which degradation processes have started. Four of 17  
 291 specimens examined (23%) had one or more bacteria of various sizes inside their degradation  
 292 vacuoles next to sediment particles (Fig 6 c, f).



293

Figure 6 TEM micrographs of *N. labradorica* showing degradation vacuoles containing miscellaneous items, including bacteria (b), inorganics (clay platelets) and unidentifiable remains after 4h incubation (a,b; specimens E27, E28, respectively); after 8h incubation (c,d; specimen E14), after 20h incubation (e,f; specimens E36, E37, respectively). v=vacuole, dv=degradation vacuole, c=kleptoplast, p=peroxisome, m=mitochondrion, li=lipid, g= Golgi. Scales: (a, c-f) 1 µm, (b) 2 µm.

### 294 3.4. Foraminiferal genetics

295 Six of 13 specimens analyzed for genetics were positively amplified and sequenced (Fig. S4). The  
 296 sequences are deposited in GenBank under the accession numbers MN514777 to MN514782.  
 297 When comparing them via BLAST, they were between 98.6% and 99.6% identical to published



298 sequences belonging to foraminifera identified as the morphospecies *N. labradorica*, from the  
299 Skagerrak, Svalbard and the White Sea (Holzmann and Pawlowski, 2017; Jauffrais et al., 2019b).  
300 Sequences were also included in an alignment comprising other nonionids implemented in  
301 Seaview (not shown) and corrected manually to check the BLAST search. This step confirmed the  
302 BLAST identification.

## 303 **4. Discussion**

### 304 **4.1. Sampling site and geochemistry**

305 The sampling site of blade corer BLC18 was in close proximity (~50 m) to an active methane-vent  
306 releasing methane bubbles at the gas hydrate pingo (GHP3) (Serov et al., 2017). At such sites with  
307 high methane fluxes, the SMTZ (sulfate methane transition zone) is shallow, as sulfate in the  
308 sediment is readily consumed in the first tens of centimeters (Barnes and Goldberg, 1976; Iversen  
309 and Jørgensen, 1993) by sulfate-reducing bacteria (SRB) (reviewed in Carrier et al., 2020).  
310 Geochemical analysis of PUC2 revealed an SMTZ at app. 13 cm, which is rather shallow (Egger  
311 et al., 2018), as it can also be several meters deep in other sites (reviewed in Panieri et al., 2017).  
312 Similar geochemical characteristics can be considered at the sampling location of living specimens  
313 (BLC18) given the close proximity of the two locations.

### 314 **4.2. Possible association with putative methanotrophs**

315 The possible association of *N. labradorica* with methanotrophs was documented via presence of  
316 two putative methanotrophs, based on microbial ultrastructure (Tavormina et al., 2015). The  
317 documentation of this possible association with putative methanotrophs likely is due to the feeding  
318 experiment. However, there is a small possibility that the associated methanotrophs were field-  
319 remains. Our results are similar to observations on field-collected *Melonis barleeanus* (Bernhard  
320 and Panieri, 2018), where a putative association with methanotrophs was described. However, the  
321 non-selective deposit-feeding behavior of *N. labradorica*, which we describe for this species for  
322 the first time, shows that methanotrophs may be ingested via untargeted grazing.

### 323 **4.3. Degradation vacuoles show large number of sediment particles and few bacteria**

324 Our results of the feeding experiment show that 23% of the examined *N. labradorica* specimens  
325 contained bacteria inside their degradation vacuoles. That is not a large proportion compared to  
326 presence of sediment particles, which occurred in 100% of the examined foraminifers. From this

327 result, however, we infer that *N. labradorica* at this site is a deposit feeder, feeding on organic  
328 detritus and associated bacteria. The bacteria observed in the degradation vacuoles resembled those  
329 from other deep-sea foraminifera (*Globobulimina pacifica* and *Uvigerina peregrina*) and the  
330 shallow-dwelling genus *Ammonia* (Goldstein and Corliss, 1994). Salt-marsh foraminifera also  
331 feed on bacteria and detritus, as observed in TEM studies (Frail-Gauthier et al., 2019). Scavenging  
332 on bacteria has also been observed by other foraminifera from intertidal environments such as  
333 *Ammonia tepida* or *Haynesina germanica* (Pascal et al., 2008) and is a logical consequence from  
334 detritus feeding. Certain foraminifera have been shown to selectively ingest algae/bacteria  
335 according to strain (Lee et al., 1966; Lee and Muller, 1973). From laboratory cultures we know  
336 that several foraminifera cultures require bacteria to reproduce, as antibiotics inhibited  
337 reproduction (Muller and Lee, 1969). Future studies will need to employ additional molecular tools  
338 to determine the food contents inside the cytoplasm (e.g. Salonen et al., 2019). A recent study used  
339 metabarcoding to assess the contribution of eukaryotic OTUs associated with intertidal  
340 foraminifera, revealing that *Ammonia* sp. T6 preys on metazoans, whereas *Elphidium* sp. S5 and  
341 *Haynesina* sp. S16 were more likely to ingest diatoms (Chronopoulou et al., 2019).

#### 342 **4.4. General ultrastructure of *N. labradorica* collected in a seep environment**

343 Our observations also included the intact nature of all major organelle types of this species, as this  
344 was essential to conclude vitality after the experiment (Nomaki et al., 2016). Mitochondria and  
345 kleptoplasts were generally homogeneously distributed throughout the cytoplasm confirming  
346 previous observations of six *N. labradorica* from the Gullmar Fjord (Lekieffre et al., 2018;  
347 Jauffrais et al., 2019b). If mitochondria are concentrated predominately under pore plugs, it can  
348 be an indicator that the electron acceptor oxygen is scarce in their environment, as the pores are  
349 the direct connection from the cell to the environment. This has been observed in several other  
350 studies where mitochondria were accumulated under pores in *N. stella* (Leutenegger and Hansen,  
351 1979) and *Bolivina pacifica* (Bernhard et al., 2010).

352 Even though our study did not focus on kleptoplasts, we could observe that kleptoplasts were  
353 occasionally degraded, which could have happened; a) during sampling, b) due to exposure to  
354 microscope lights or c) due to the age and condition of kleptoplasts inside the host. Kleptoplasts  
355 in *N. labradorica* have been studied in detail describing their diatom origin (Cedhagen, 1991),  
356 sensitivity to light and missing photosynthetic functionality (Jauffrais et al., 2019b). Kleptoplasts  
357 in *Elphidium williamsoni* might have an value for providing extra carbon storage and calls the need

358 for more studies on complex feeding strategies developed by kleptoplastic foraminifera  
359 (Jauffrais et al., 2019a).

## 360 **5. Conclusions**

361 Based on the content of degradation vacuoles, we conclude that *N. labradorica* from our study  
362 site, an active methane emitting site in the Barents Sea, is a deposit-feeder. It ingests large  
363 amounts of sediment particles together with bacteria. On two specimens of the feeding experiment,  
364 putative methanotrophs were observed near the *N. labradorica* aperture, suggesting ingestion of  
365 *M. sedimenti* via “untargeted grazing”. Further studies are needed on feeding strategies of other  
366 paleo-oceanographically relevant foraminifera to detangle the relationship between  $\delta^{13}\text{C}$  of  
367 foraminiferal calcite, their cytoplasm and dietary composition.

## 368 **6. Data availability**

369 Data in form of TEM images will be deposited at PANGAEA (doi)

370 Molecular data is deposited at Genbank (doi)

## 371 **7. Sample availability**

372 Samples are available upon request and TEM thinsections archived at the University of Angers.

## 373 **8. Acknowledgments**

374 We thank the captains, crew members and scientists onboard R/V *Kronprins Haakon* and ROV  
375 *Ægir* Team for their assistance; Anne-Grethe Hestnes for growing the methanotroph culture.  
376 Florence Manero, Romain Mallet and Rodolphe Perrot at the SCIAM microscopy facility  
377 University of Angers are to thank for their expertise with the TEM and SEM. We thank Sunil  
378 Vadakkepuliambatta for helping to prepare the map presented in Figure 1; Sophie Quinchart  
379 (LPG-BIAF) for supporting the molecular analysis. Funding was received through the Research  
380 Council of Norway, CAGE (Center for Excellence in Arctic Gas Hydrate Environment and  
381 Climate, project number 223259) and NORCRUST (project number 255150) to GP, EG, and CS.  
382 CS position was funded through the MOPGA (Make Our Planet Great Again) fellowship by  
383 CAMPUS France, the NORCRUST project and the University of Angers. JMB was partially  
384 supported by US NSF 1634469, WHOI’s Investment in Science Program, and by the Région Pays  
385 de la Loire through the FRESCO Project.

386 **Author Contributions**

387 Designed the project and experiment: GP, EG, CS; Collected samples: CS, EG; Performed  
388 experiment: CS; Sample preparation: CS, HR; TEM observations and interpretations: CS, JMB,  
389 EG, CL; Conducted molecular genetics: MSc; Wrote the paper: CS, GP, JMB; Provided critical  
390 review and edits to the manuscript: EG, CL, MSv, MSc, HR; Contributed  
391 reagents/materials/analysis tools: MSv, MSc, CL.

392

393 **Table I.** Summary of TEM observations of *Nonionellina labradorica* comparing field specimens  
 394 and experimental specimens. Field specimens (initials) were not fed, nor was a non-fed control  
 395 preserved after a 20 h incubation. The only putative methanotrophs were observed and imaged in  
 396 specimens from the 20 h incubation. Bacteria of unknown origin were described as rod shaped  
 397 cells in the degradation vacuoles.  
 398

Duration of experiment (h)/field samples	Food provided (yes (x)/no)	Sample ID	Cytoplasm: Degradation vacuole Contents		Aperture region: (putative) Methanotrophs
			bacteria	Clay/in-organics	
Field samples (Initials)	No	E1	no	x	no
	No	E3	no	x	no
	No	E5	no	x	no
	No	E6	no	x	no
4	x	E25	no	x	no
	x	E27	x	x	no
	x	E28	no	x	no
	x	E29	no	x	no
8	x	E14	x	x	no
	x	E15	no	x	no
	x	E16	no	x	no
	x	E17	no	x	no
20	x	E36	x	x	1 x
	x	E37	x	x	no
	x	E38	no	x	no
	x	E39	no	x	2 x
Control (20)	no	E44	no	x	no

399  
 400  
 401

402 **References:**

403

404 Altschul, S. F., Madden, T. L., Schäffer, A. A., Zhang, J., Zhang, Z., Miller, W., and Lipman, D.  
405 J.: Gapped BLAST and PSI-BLAST: a new generation of protein database search programs,  
406 *Nucleic Acids Res.*, 25, 3389-3402, <https://doi.org/10.1093/nar/25.17.3389>, 1997.

407 Barnes, R. O. and Goldberg, E. D.: Methane production and consumption in anoxic marine  
408 sediments, *Geology*, 4, 297-300, [https://doi.org/10.1130/0091-  
409 7613\(1976\)4<297:MPACIA>2.0.CO;2](https://doi.org/10.1130/0091-7613(1976)4<297:MPACIA>2.0.CO;2), 1976.

410 Bé, A. W. H., Spero, H. J., and Anderson, O. R.: Effects of symbiont elimination and reinfection  
411 on the life processes of the planktonic foraminifer *Globigerinoides sacculifer*, *Marine Biology*,  
412 70, 73-86, <https://doi.org/10.1007/BF00397298>, 1982.

413 Bernhard, J. M. and Bowser, S. S.: Benthic foraminifera of dysoxic sediments: chloroplast  
414 sequestration and functional morphology, *Earth-Sci. Rev.*, 46, 149-165,  
415 [https://doi.org/10.1016/s0012-8252\(99\)00017-3](https://doi.org/10.1016/s0012-8252(99)00017-3), 1999.

416 Bernhard, J. M. and Panieri, G.: Keystone Arctic paleoceanographic proxy association with  
417 putative methanotrophic bacteria, *Sci Rep-Uk*, 8, 10610, [https://doi.org/10.1038/s41598-018-  
418 28871-3](https://doi.org/10.1038/s41598-018-28871-3), 2018.

419 Bernhard, J. M., Goldstein, S. T., and Bowser, S. S.: An ectobiont-bearing foraminiferan,  
420 *Bolivina pacifica*, that inhabits microxic pore waters: cell-biological and paleoceanographic  
421 insights, *Environmental Microbiology*, 12, 2107-2119, 10.1111/j.1462-2920.2009.02073.x,  
422 2010.

423 Carrier, V., Svenning, M. M., Gründger, F., Niemann, H., Dessandier, P.-A., Panieri, G., and  
424 Kalenitchenko, D.: The Impact of Methane on Microbial Communities at Marine Arctic Gas  
425 Hydrate Bearing Sediment, *Frontiers in Microbiology*, 11, 10.3389/fmicb.2020.01932, 2020.

426 Cedhagen, T.: Retention of chloroplasts and bathymetric distribution in the sublittoral  
427 foraminiferan *Nonionellina labradorica*, *Ophelia*, 33, 17-30,  
428 <https://doi.org/10.1080/00785326.1991.10429739>, 1991.

429 Charrieau, L. M., Ljung, K., Schenk, F., Daewel, U., Kritzberg, E., and Filipsson, H. L.: Rapid  
430 environmental responses to climate-induced hydrographic changes in the Baltic Sea entrance,  
431 *Biogeosciences*, 16, 3835-3852, 10.5194/bg-16-3835-2019, 2019.

432 Choquel, C., Geslin, E., Metzger, E., Filipsson, H. L., Risgaard-Petersen, N., Launeau, P.,  
433 Giraud, M., Jauffrais, T., Jesus, B., and Mouret, A.: Denitrification by benthic foraminifera and  
434 their contribution to N-loss from a fjord environment, *Biogeosciences*, 18, 327-341, 10.5194/bg-  
435 18-327-2021, 2021.

- 436 Chronopoulou, P.-M., Salonen, I., Bird, C., Reichart, G.-J., and Koho, K. A.: Metabarcoding  
437 insights into the trophic behavior and identity of intertidal benthic foraminifera, *Frontiers in*  
438 *microbiology*, 10, 1169, <https://doi.org/10.3389/fmicb.2019.01169>, 2019.
- 439 Consolaro, C., Rasmussen, T., Panieri, G., Mienert, J., Bünz, S., and Sztybor, K.: Carbon isotope  
440 ( $\delta^{13}\text{C}$ ) excursions suggest times of major methane release during the last 14 kyr in Fram Strait,  
441 the deep-water gateway to the Arctic, *Clim. Past*, 11, 669-685, [https://doi.org/10.5194/cp-11-](https://doi.org/10.5194/cp-11-669-2015)  
442 [669-2015](https://doi.org/10.5194/cp-11-669-2015), 2015.
- 443 Darling, K. F., Schweizer, M., Knudsen, K. L., Evans, K. M., Bird, C., Roberts, A., Filipsson, H.  
444 L., Kim, J.-H., Gudmundsson, G., Wade, C. M., Sayer, M. D. J., and Austin, W. E. N.: The  
445 genetic diversity, phylogeography and morphology of Elphidiidae (Foraminifera) in the  
446 Northeast Atlantic, *Mar. Micropaleontol.*, 129, 1-23,  
447 <https://doi.org/10.1016/j.marmicro.2016.09.001>, 2016.
- 448 Dessandier, P.-A., Borrelli, C., Kalenitchenko, D., and Panieri, G.: Benthic Foraminifera in  
449 Arctic Methane Hydrate Bearing Sediments, *Frontiers in Marine Science*, 6,  
450 <https://doi.org/10.3389/fmars.2019.00765>, 2019.
- 451 Egger, M., Riedinger, N., Mogollón, J. M., and Jørgensen, B. B.: Global diffusive fluxes of  
452 methane in marine sediments, *Nature Geoscience*, 11, 421-425, 10.1038/s41561-018-0122-8,  
453 2018.
- 454 Fossile, E., Nardelli, M. P., Jouini, A., Lansard, B., Pusceddu, A., Moccia, D., Michel, E., Péron,  
455 O., Howa, H., and Mojtahid, M.: Benthic foraminifera as tracers of brine production in  
456 Storfjorden “sea ice factory”, *Biogeosciences*, 17, <https://doi.org/10.5194/bg-17-1933-2020>,  
457 2020.
- 458 Frail-Gauthier, J. L., Mudie, P. J., Simpson, A. G. B., and Scott, D. B.: Mesocosm and  
459 Microcosm Experiments On the Feeding of Temperate Salt Marsh Foraminifera, *J. Foraminifer.*  
460 *Res.*, 49, 259-274, <https://doi.org/10.2113/gsjfr.49.3.259>, 2019.
- 461 Goldstein, S. T. and Corliss, B. H.: Deposit feeding in selected deep-sea and shallow-water  
462 benthic foraminifera, *Deep Sea Research Part I: Oceanographic Research Papers*, 41, 229-241,  
463 [https://doi.org/10.1016/0967-0637\(94\)90001-9](https://doi.org/10.1016/0967-0637(94)90001-9), 1994.
- 464 Gouy, M., Guindon, S., and Gascuel, O.: SeaView version 4: a multiplatform graphical user  
465 interface for sequence alignment and phylogenetic tree building, *Mol. Biol. Evol.*, 27, 221-224,  
466 <https://doi.org/10.1093/molbev/msp259>, 2010.
- 467 Hald, M. and Korsun, S.: Distribution of modern benthic foraminifera from fjords of Svalbard,  
468 European Arctic, *The Journal of Foraminiferal Research*, 27, 101-122,  
469 <https://doi.org/10.2113/gsjfr.27.2.101>, 1997.

- 470 Heinz, P., Geslin, E., and Hemleben, C.: Laboratory observations of benthic foraminiferal cysts,  
471 Mar. Biol. Res., 1, 149-159, 2005.
- 472 Hemleben, C., Spindler, M., and Anderson, O. R.: Modern planktonic foraminifera, Springer  
473 Science & Business Media 2012.
- 474 Herguera, J. C., Paull, C. K., Perez, E., Ussler Iii, W., and Peltzer, E.: Limits to the sensitivity of  
475 living benthic foraminifera to pore water carbon isotope anomalies in methane vent  
476 environments, Paleoceanography, 29, 273-289, <https://doi.org/10.1002/2013PA002457>, 2014.
- 477 Hill, R., Schreiber, U., Gademann, R., Larkum, A. W. D., Kuhl, M., and Ralph, P. J.: Spatial  
478 heterogeneity of photosynthesis and the effect of temperature-induced bleaching conditions in  
479 three species of corals, Marine Biology, 144, 633-640, [https://doi.org/10.1007/s00227-003-1226-](https://doi.org/10.1007/s00227-003-1226-1)  
480 [1](https://doi.org/10.1007/s00227-003-1226-1), 2004a.
- 481 Hill, T. M., Kennett, J. P., and Valentine, D. L.: Isotopic evidence for the incorporation of  
482 methane-derived carbon into foraminifera from modern methane seeps, Hydrate Ridge,  
483 Northeast Pacific, Geochimica et Cosmochimica Acta, 68, 4619-4627,  
484 <https://doi.org/10.1016/j.gca.2004.07.012>, 2004b.
- 485 Hinrichs, K.-U., Hmelo, L. R., and Sylva, S. P.: Molecular fossil record of elevated methane  
486 levels in late Pleistocene coastal waters, Science, 299, 1214-1217,  
487 <https://doi.org/10.1126/science.1079601>, 2003.
- 488 Holzmann, M. and Pawlowski, J.: An updated classification of rotaliid foraminifera based on  
489 ribosomal DNA phylogeny, Mar. Micropaleontol., 132, 18-34,  
490 <https://doi.org/10.1016/j.marmicro.2017.04.002>, 2017.
- 491 Hong, W.-L., Torres, M. E., Carroll, J., Crémière, A., Panieri, G., Yao, H., and Serov, P.:  
492 Seepage from an arctic shallow marine gas hydrate reservoir is insensitive to momentary ocean  
493 warming, Nat. Commun., 8, 15745, <https://doi.org/10.1038/ncomms15745>, 2017.
- 494 Hong, W. L., Torres, M. E., Portnov, A., Waage, M., Haley, B., and Lepland, A.: Variations in  
495 gas and water pulses at an Arctic seep: fluid sources and methane transport, Geophys. Res. Lett.,  
496 45, 4153-4162, <https://doi.org/10.1029/2018GL077309>, 2018.
- 497 Iversen, N. and Jørgensen, B. B.: Diffusion coefficients of sulfate and methane in marine  
498 sediments: Influence of porosity, Geochimica et Cosmochimica Acta, 57, 571-578,  
499 [https://doi.org/10.1016/0016-7037\(93\)90368-7](https://doi.org/10.1016/0016-7037(93)90368-7), 1993.
- 500 Jauffrais, T., LeKieffre, C., Schweizer, M., Jesus, B., Metzger, E., and Geslin, E.: Response of a  
501 kleptoplastidic foraminifer to heterotrophic starvation: photosynthesis and lipid droplet  
502 biogenesis, FEMS Microbiol. Ecol., 95, 10.1093/femsec/fiz046, 2019a.



- 503 Jauffrais, T., LeKieffre, C., Schweizer, M., Geslin, E., Metzger, E., Bernhard, J. M., Jesus, B.,  
504 Filipsson, H. L., Maire, O., and Meibom, A.: Kleptoplastidic benthic foraminifera from aphotic  
505 habitats: insights into assimilation of inorganic C, N and S studied with sub-cellular resolution,  
506 *Environmental microbiology*, 21, 125-141, <https://doi.org/10.1111/1462-2920.14433>, 2019b.
- 507 Lee, J. J. and Muller, W. A.: Trophic dynamics and niches of salt marsh foraminifera, *Am. Zool.*,  
508 13, 215-223, 1973.
- 509 Lee, J. J., McEnery, M., Pierce, S., Freudenthal, H., and Muller, W.: Tracer experiments in  
510 feeding littoral foraminifera, *The Journal of Protozoology*, 13, 659-670, 1966.
- 511 LeKieffre, C., Bernhard, J. M., Mabilieu, G., Filipsson, H. L., Meibom, A., and Geslin, E.: An  
512 overview of cellular ultrastructure in benthic foraminifera: New observations of rotalid species in  
513 the context of existing literature, *Mar. Micropaleontol.*, 138, 12-32,  
514 <https://doi.org/10.1016/j.marmicro.2017.10.005>, 2018.
- 515 Leutenegger, S. and Hansen, H. J.: Ultrastructural and radiotracer studies of pore function in  
516 foraminifera, *Marine Biology*, 54, 11-16, 10.1007/BF00387046, 1979.
- 517 Lipps, J. H.: Biotic Interactions in Benthic Foraminifera, in: *Biotic Interactions in Recent and*  
518 *Fossil Benthic Communities*, edited by: Tevesz, M. J. S., and McCall, P. L., Springer US,  
519 Boston, MA, 331-376, 10.1007/978-1-4757-0740-3\_8, 1983.
- 520 Mackensen, A.: On the use of benthic foraminiferal  $\delta^{13}\text{C}$  in palaeoceanography: constraints  
521 from primary proxy relationships, *Geological Society, London, Special Publications*, 303, 121-  
522 133, <https://doi.org/10.1144/SP303.9>, 2008.
- 523 Mojtahid, M., Zubkov, M. V., Hartmann, M., and Gooday, A. J.: Grazing of intertidal benthic  
524 foraminifera on bacteria: Assessment using pulse-chase radiotracing, *J. Exp. Mar. Biol. Ecol.*,  
525 399, 25-34, <https://doi.org/10.1016/j.jembe.2011.01.011>, 2011.
- 526 Muller, W. A. and Lee, J. J.: Apparent Indispensability of Bacteria in Foraminiferan Nutrition,  
527 *The Journal of Protozoology*, 16, 471-478, <https://doi.org/10.1111/j.1550-7408.1969.tb02303.x>,  
528 1969.
- 529 Nomaki, H., Heinz, P., Nakatsuka, T., Shimanaga, M., and Kitazato, H.: Species-specific  
530 ingestion of organic carbon by deep-sea benthic foraminifera and meiobenthos: In situ tracer  
531 experiments, *Limnol. Oceanogr.*, 50, 134-146, <https://doi.org/10.4319/lo.2005.50.1.0134>, 2005.
- 532 Nomaki, H., Heinz, P., Nakatsuka, T., Shimanaga, M., Ohkouchi, N., Ogawa, N. O., Kogure, K.,  
533 Ikemoto, E., and Kitazato, H.: Different ingestion patterns of C-13-labeled bacteria and algae by  
534 deep-sea benthic foraminifera, *Marine Ecology-Progress Series*, 310, 95-108,  
535 <https://doi.org/10.3354/meps310095>, 2006.

- 536 Nomaki, H., Bernhard, J. M., Ishida, A., Tsuchiya, M., Uematsu, K., Tame, A., Kitahashi, T.,  
537 Takahata, N., Sano, Y., and Toyofuku, T.: Intracellular Isotope Localization in *Ammonia* sp.  
538 (*Foraminifera*) of Oxygen-Depleted Environments: Results of Nitrate and Sulfate Labeling  
539 Experiments, *Frontiers in Microbiology*, 7, <https://doi.org/10.3389/fmicb.2016.00163>, 2016.
- 540 Panieri, G.: Foraminiferal response to an active methane seep environment: A case study from  
541 the Adriatic Sea, *Mar. Micropaleontol.*, 61, 116-130,  
542 <https://doi.org/10.1016/j.marmicro.2006.05.008>, 2006.
- 543 Panieri, G., James, R. H., Camerlenghi, A., Westbrook, G. K., Consolaro, C., Cacho, I., Cesari,  
544 V., and Cervera, C. S.: Record of methane emissions from the West Svalbard continental margin  
545 during the last 23.500yrs revealed by  $\delta^{13}\text{C}$  of benthic foraminifera, *Global and Planetary*  
546 *Change*, 122, 151-160, <https://doi.org/10.1016/j.gloplacha.2014.08.014>, 2014.
- 547 Panieri, G., Lepland, A., Whitehouse, M. J., Wirth, R., Raanes, M. P., James, R. H., Graves, C.  
548 A., Crémière, A., and Schneider, A.: Diagenetic Mg-calcite overgrowths on foraminiferal tests in  
549 the vicinity of methane seeps, *Earth and Planetary Science Letters*, 458, 203-212,  
550 <https://doi.org/10.1016/j.epsl.2016.10.024>, 2017.
- 551 Pascal, P.-Y., Dupuy, C., Richard, P., and Niquil, N.: Bacterivory in the common foraminifer  
552 *Ammonia tepida*: Isotope tracer experiment and the controlling factors, *J. Exp. Mar. Biol. Ecol.*,  
553 359, 55-61, <https://doi.org/10.1016/j.jembe.2008.02.018>, 2008.
- 554 Pawlowski, J.: Introduction to the molecular systematics of foraminifera, *Micropaleontology*, 46,  
555 1-12, 2000.
- 556 Rathburn, A. E., Pérez, M. E., Martin, J. B., Day, S. A., Mahn, C., Gieskes, J., Ziebis, W.,  
557 Williams, D., and Bahls, A.: Relationships between the distribution and stable isotopic  
558 composition of living benthic foraminifera and cold methane seep biogeochemistry in Monterey  
559 Bay, California, *Geochemistry, Geophysics, Geosystems*, 4, 2003.
- 560 Risgaard-Petersen, N., Langezaal, A. M., Ingvarnsen, S., Schmid, M. C., Jetten, M. S. M., Op  
561 den Camp, H. J. M., Derksen, J. W. M., Piña-Ochoa, E., Eriksson, S. P., Peter Nielsen, L., Peter  
562 Revsbech, N., Cedhagen, T., and van der Zwaan, G. J.: Evidence for complete denitrification in a  
563 benthic foraminifer, *Nature*, 443, 93, <https://doi.org/10.1038/nature05070>, 2006.
- 564 Salonen, I. S., Chronopoulou, P.-M., Bird, C., Reichart, G.-J., and Koho, K. A.: Enrichment of  
565 intracellular sulphur cycle-associated bacteria in intertidal benthic foraminifera revealed by 16S  
566 and *aprA* gene analysis, *Sci Rep-Uk*, 9, 1-12, <https://doi.org/10.1038/s41598-019-48166-5>, 2019.
- 567 Schneider, A., Crémière, A., Panieri, G., Lepland, A., and Knies, J.: Diagenetic alteration of  
568 benthic foraminifera from a methane seep site on Vestnesa Ridge (NW Svalbard), *Deep Sea*  
569 *Research Part I: Oceanographic Research Papers*, 123, 22-34,  
570 <https://doi.org/10.1016/j.dsr.2017.03.001>, 2017.

- 571 Serov, P., Vadakkepuliambatta, S., Mienert, J., Patton, H., Portnov, A., Silyakova, A., Panieri,  
572 G., Carroll, M. L., Carroll, J., Andreassen, K., and Hubbard, A.: Postglacial response of Arctic  
573 Ocean gas hydrates to climatic amelioration, *Proceedings of the National Academy of Sciences*,  
574 114, 6215-6220, [10.1073/pnas.1619288114](https://doi.org/10.1073/pnas.1619288114), 2017.
- 575 Shetye, S., Mohan, R., Shukla, S. K., Maruthadu, S., and Ravindra, R.: Variability of  
576 *Nonionellina labradorica* Dawson in Surface Sediments from Kongsfjorden, West Spitsbergen,  
577 *Acta Geologica Sinica - English Edition*, 85, 549-558, [https://doi.org/10.1111/j.1755-  
578 6724.2011.00450.x](https://doi.org/10.1111/j.1755-6724.2011.00450.x), 2011.
- 579 Tavormina, P. L., Hatzepichler, R., McGlynn, S., Chadwick, G., Dawson, K. S., Cannon, S. A.,  
580 and Orphan, V. J.: *Methyloprofundus sedimenti* gen. nov., sp. nov., an obligate methanotroph  
581 from ocean sediment belonging to the 'deep sea-1' clade of marine methanotrophs, *Int. J. Syst.*  
582 *Evol. Microbiol.*, 65, 251-259, <https://doi.org/10.1099/ijs.0.062927-0>, 2015.
- 583 Torres, M. E., Martin, R. A., Klinkhammer, G. P., and Nesbitt, E. A.: Post depositional alteration  
584 of foraminiferal shells in cold seep settings: New insights from flow-through time-resolved  
585 analyses of biogenic and inorganic seep carbonates, *Earth and Planetary Science Letters*, 299,  
586 10-22, <https://doi.org/10.1016/j.epsl.2010.07.048>, 2010.
- 587 Wefer, G., Heinze, P. M., and Berger, W. H.: Clues to ancient methane release, *Nature*, 369, 282,  
588 <https://doi.org/10.1038/369282a0>, 1994.
- 589 Wollenburg, J. E., Raitzsch, M., and Tiedemann, R.: Novel high-pressure culture experiments on  
590 deep-sea benthic foraminifera—Evidence for methane seepage-related  $\delta^{13}\text{C}$  of *Cibicides*  
591 *wuellerstorfi*, *Mar. Micropaleontol.*, 117, 47-64, 2015.
- 592